University of Tehran Press

Journal of the Earth and Space Physics

Homepage: https://jesphys.ut.ac.ir

Vol. 48, No. 4, Winter 2023, P. 125-135
(Research Article)

Calibration of IASPEI Standard Broad-band Magnitude m_B for Iranian Plateau Earthquakes

Kiani, M.[1] | Moradi, A.[2]

1. Department of Seismology, Institute of Geophysics, University of Tehran, Tehran, Iran. E-mail: mehran.kiani@alumni.ut.ac.ir
2. **Corresponding Author**, Department of Seismology, Institute of Geophysics, University of Tehran, Tehran, Iran. E-mail: asmoradi@ut.ac.ir

(Received: 26 June 2022, Revised: 1 Aug 2022, Accepted: 4 Oct 2022, Published online: 5 March 2023)

Abstract

Located in Alp-Himalayan belt and an active tectonic plate, Iran is annually struck by major earthquakes. Since shallow earthquakes cause considerable loss of lives and property in this region, using any method to decrease the time of magnitude estimation of great earthquakes is very important for making a prompt decision about what to do. To achieve this aim, m_B was computed as a rapid estimator for 38 earthquakes with magnitudes greater than 6 occurred in Iran and adjacent areas (24°-44°N, 42°-66°E) from 1990 to 2018. The magnitudes that estimated by using the calibration function by Saul & Bormann (2007) have a standard error of 0.49 from Mw (in this study). Therefore, m_B's calibration function was modified. As a result, the magnitudes obtained are approximately equal to those of reported Mw (a standard error of 0.18). The calibration function acquired in this study for Iran's earthquakes is lower than the m_B's global calibration function obtained by Saul & Bormann (2007). Their difference is nearly one unit at short distances, which can be related to the earthquakes located in subduction zones and plates boundaries used by Saul & Bormann (2007) that systemically have lower stress drops than intraplate earthquakes considered here. Thus it is needed to develop improved region-specific calibration functions for m_B. However, the difference became smaller at distances greater than 20°. Consequently, this method and new calibration function can be employed to estimate magnitudes as early as possible across Iran plateau.

Keywords: m_B, M_w, Earthquake Magnitude, Calibration, Iran Plateau.

1. Introduction

One of the most significant reasons why magnitudes must be rapidly estimated is the necessity of rapid and accurate estimation of the location and magnitude of earthquakes for taking appropriate disaster management actions. Major earthquakes hit large cities of Iran on a yearly basis with a potential toll of hundreds of lives. These earthquakes can completely destroy a lot of buildings or heritage sites and cause severe damages to the local economy. To exemplify, 1990 is remembered for the great earthquake that destroyed Manjil and Rudbär. The earthquake, which measured 7.4 on the moment magnitude scale, made more than 500,000 people homeless and caused 13,000-40,000 deaths. It has been known as the largest instrumentally recorded event in the Alborz Mountains of northern Iran and is related to a range-parallel left-lateral strike-slip with surface rupture of ~80 km (Berberian & Walker, 2010). Similarly, several earthquakes frequently occurred in Iran such as May 1, 1997 in Ghaen, December 26, 2003 in Bam, August 11, 2012 in Varzaghan and November 17, 2017 in Azgeleh.

As a result of rapid population growth in the earthquake-prone cities of Iran, rapid estimation of earthquake magnitude plays a vital role in aid procedures and emergency responses. In Iran, the Iranian Seismological Center (IRSC) is officially responsible for analyzing earthquakes and providing governmental organizations with reports on a regular basis. Rapid location and estimation of earthquake parameters are key issues for the center. To address the issues, an effective method needs to be employed to estimate earthquake magnitude as early as possible. Many researchers try to find a method to rapidly estimate the magnitude of large

Cite this article: Kiani, M., & Moradi, A. (2023). Calibration of IASPEI Standard Broad-band Magnitude m_B for Iranian Plateau Earthquakes. *Journal of the Earth and Space Physics*, 48(4), 125-135. DOI: http//doi.org/10.22059/jesphys.2022.345010.1007444

Publisher: University of Tehran Press.
DOI: http//doi.org/10.22059/jesphys.2022.345010.1007444

Print ISSN: 2538-371X
Online ISSN: 2538-3906

earthquakes, especially after Sumatra's great earthquake (2004). Although the best and most common method for magnitude estimation is determination of moment magnitude M_w (Hanks & Kanamori, 1979), it is a time-consuming process because it can be determined by seismic moment that is routinely determined by centroid moment tensor inversion based on regional or teleseismic waveform modeling (e.g. Swiss Federal Institute of Technology in Zurich (SED/ETHZ), Global Moment Tensor Catalog (GCMT)). The moment magnitude comes from long-period moment tensor determination including global centroid moment tensor (M_w^{GCMT}) (Dziewonski et al., 1981; Ekström et al., 2012).

Seismologists make an effort to adopt a simpler and less complex method to estimate earthquake magnitude as early and precisely as possible. Therefore, a rapid and reliable estimation of seismic moment is recently available from 5 to 15 min after OT in the regions that were equipped with a dense network. Several procedures have also been designed to estimate great earthquake magnitudes rapidly. These procedures are currently used in earthquake and tsunami monitoring systems.

Duputel & Hayes (2012), Hayes et al. (2009), and Kanamori & Rivera (2008) used W phase, which corresponds to the superposition of the first overtones of the Earth normal modes between 100s and 1000s (Duputel et al., 2012), Kanamori, 1993), at teleseismic distances for a source inversion algorithm. The W phase source inversion algorithm is now running online at U.S. Geological Survey (USGS), at the Pacific Tsunami Warning Center (NOAA/NWS/PTWC) and at the Institute de Physique du Globe de Strasbourg (IPGS-EOST, CNRS/UdS). The W phase solution calculated at PTWC is issued internally within 30 minutes after origin time (O.T.) in order to have a quick preliminary robust estimate of the event magnitude and focal mechanism of large earthquakes.

M_m is another method that is computed from spectral amplitude of mantle Rayleigh waves at variable periods (between 50 and 300 seconds for great events) combined with approximate correction for geometrical spreading (Lomax & Michelini, 2005; Weinstein & Okal, 2005; Newman & Okal, 1998; Okal & Talandier, 1989). Thus, great earthquakes can be manually recorded and reported 5-30 minutes after OT, which should be optimally shortened. A simple and fast method is required to estimate the magnitude accurately as early as possible. The methods of using P-wave in local and regional distances that are rapid and accurate.

The first signals that arrive at a seismic station are seismic P waves. Also, the initial P waves and their following wave trains have useful information about size and source parameters of events. These justify the earthquake use of initial P waves to estimate the magnitude. Boatwright & Choy (1986) came to the conclusion that total seismic energy radiated can be estimated from only the P-wave train.

One of the procedures that initial P-wave is used to estimate the magnitude is U.S. Geological Survey National Earthquake Center's (NEIC) Fast Moment Tensor (Sipkin, 1994, USGS), for the magnitude of 5.5 or greater within 30 minutes after OT through the inversion of P-wave train. Another P-wave procedure is M_{wp} (Tsuboi 2000; Tsuboi et al., 1999, 1995), which considers very-broad-band, P-wave seismograms as approximate far-field, source time functions. The integrated and corrected approximation for geometrical spreading and an average radiation pattern can be used for obtaining scalar moments at each station. Averaging over stations and optionally applying a magnitude-dependent correction (Whitmore et al., 2002) gives the moment magnitude, M_{wp}. Lomax & Michelini (2005) suggest that the high frequency P-wave duration can be used for rapid estimation of the magnitude. Lomax et al. (2007) used teleseismic P-wave signals to estimate radiated seismic energy and source duration, and showed that an energy-duration moment relation, based on an expression from Vassiliou & Kanamori (1982), gives a moment magnitude, M_{ED}. Furthermore, Lomax & Michelini (2009) introduced rapid determination of moment magnitude, M_{wpd}, using large earthquakes P-waves, recording at teleseismic distances and applying the duration-amplitude method procedure.

The Working Group on Magnitudes of the International Association of Seismology and

Physics of the Earth Interior (IASPEI) Commission on Seismological Observation and Interpretation for the generic intermediate-period/broadband body-wave magnitude m_B proposes a procedure based on the maximum amplitude of the P-wave measured on a velocity-proportional trace denoting m_B (BB).

This procedure requires the use of unfiltered broad-band (BB) records that are proportional to ground motion velocity. According to this standard, the measurement time window for m_B must contain the largest amplitude of the P-wave train, including P, pP, sP, and possibly PcP and their codas, but end preferably before PP. m_B is the original Gutenberg (1945) body-wave magnitude measured on relatively broadband medium-period instrument at periods between 2s and 20s. IASPEI standard procedure for calculation of m_B(BB) uses the vertical component P-wave of Gutenberg & Richter (1956) calibration function and broadens the period range to 0.2s < T < 30s. Although the global standards do not yet propose to calculate body-wave magnitude at distances less than 20°, Saul & Bormann (2007) have derived a much smoother distance dependence of vertical component P-wave calibration function for distances below 20° from global velocity broadband amplitude measurements. Bormann & Saul (2008) illustrated a simple method to find the appropriate time window to search for the maximum P-amplitude that reduces the magnitude estimation time to 2 minutes after OT for regional earthquake with a magnitude between 6 and 7.

Bormann & Saul (2009), Bormann et al. (2006), Bormann & Wylegalla (2005) calculated a cumulative m_B (broad-band body-wave magnitude (m_{Bc})) based on Bormann & Khalturin (1975). Their calculations were done by summing up the peak velocity amplitude between two adjacent zero crossings in P-wave combined with distance correction using Saul & Bormann (2007) Q_{pv} calibration function. In this procedure, large earthquakes P-wave records on broad-band seismograms between 5° and 105° can be used for rapid and accurate magnitude estimation. The algorithm is very simple and clear compared to other methods. Besides, magnitude estimation is available within minutes (5 minutes) after OT.

Herein, m_B was calculated based on Bormann & Saul (2008) method (as a fast and accurate magnitude estimation method) using their calibration function for 38 earthquakes with magnitudes between 6 and 7.5 in Iran and adjacent areas from 1990 to 2018. As can be seen from Table 1, there is some differences between the obtained results and reported magnitudes, M_w^{GCMT}. According to Bormann & Dewey (2014), "in general, there is a need to develop improved global and region-specific calibration functions for both m_b and m_B, or to confirm some of the various calibration functions that have already been proposed." Consequently, vertical component P-wave calibration function (Q_{pv}) was modified for Iran Plateau and adjacent areas and magnitudes for those earthquakes were recalculated by new calibration function. In conformity with Table 1, there are acceptable differences between magnitudes calculated by the new calibration function and the reported M_w^{GCMT}.

2. Methodology

IASPEI (2013) proposed a procedure based on the maximum amplitude of P-wave for the generic intermediate-period/broad-band body-wave magnitude m_B, on a velocity proportional trace and denoted it m_B (BB):

$$m_B(BB) = \log_{10}\left(^{v_{max}}/_{2\pi}\right) + Q(\Delta, h) - 3.0 \qquad (1)$$

where, V_{max} is ground velocity in nm/s associated with the maximum trace-amplitude in the entire P-phase train (time spanned by P, pP, sP, and possibly PcP and their codas, but ending preferably before PP). Also as recorded on a vertical-component seismogram that is proportional to the velocity, where the period of the measured phase, T, should satisfy the condition 0.2s < T < 30s, and where T should be preserved together with V_{max} in bulletin databases; Q(Δ, h) is attenuation function for PZ established by Gutenberg & Richter (1956); Δ is epicentral distance in degrees, 20° ≤ Δ ≤ 100°; and h = focal depth in km. This equation differs from the equation for m_B of Gutenberg & Richter (1956) by virtue of the $\log_{10}\left(^{v_{max}}/_{2}\right)$ term, which replaces the classical $\log_{10}(A/T)_{max}$ term.

According to IASPEI procedure, m_B (BB) was corrected by Gutenberg & Richter (1956) calibration function (Q_{pv}) for the distance between 21° and 100°. Saul & Bormann (2007) developed a new m_B calibration function including the distance range between 5° and 20°. Moreover, the estimated time decreases to 2 minutes after P-wave onset through the use of the new calibration function. However, the calibration function for distances between 5° and 20° is not reliable enough for global application. This issue was found much earlier by Evernden (1967).

Evernden (1967) found it necessary to adjust the distance-depth correction of Gutenberg & Richter (1956) calibration function at distances of less than 20°. Also, Chung & Bernreuter (1980) stated that the regional variation of geological factors within the earth like Q structure, physical state and the composition can have an effect on the estimation of body-wave magnitude. Consequently, as mentioned above, there is a need to develop improved global and region-specific calibration functions for m_B. Thus, the aim of this study is to modify calibration functions of m_B for regional distances, especially for Iran Plateau.

The same procedure used by Bormann & Saul (2008) was employed to estimate m_B. The process includes the following steps:

- Removing instrument response from each seismogram in order to obtain ground velocity (ms^{-1}).
- Obtaining P-wave train through cutting each seismogram from P-arrival to S in order to estimate P-wave duration.
- Estimating m_B by maximum velocity amplitude in a predetermined window and in specified periods.

An important step is the estimation of time window duration based on IASPEI (2013) to search for maximum P-amplitude. In accordance with the IASPEI procedure, the time window must preferably end before PP, but for great earthquakes with long rupture duration, significant amounts of P-wave energy can arrive after the PP arrival. As stated by Bormann & Saul (2008, 2009), to constrain the time window, one can use the duration of high-frequency radiation mainly generated at the progressing rupture front as an estimation of rupture duration. But this duration tends to be longer than rupture duration because of the deliberate inclusion of the depth phases of P and their codas. To determine the duration D (here, the term duration means the high-frequency radiation duration which should end/be ended before the arrival of S-wave) of high-frequency, this work followed the procedure used by Bormann & Saul (2008, 2009). They took advantage of the deficiency in high-frequency energy of PP (Astiz et al., 1996; Lomax et al., 2007).

As it can be seen in Bormann & Saul's (2008, 2009) computations, the average high-frequency duration they measured for an earthquake with a magnitude of M_w between 6 and 7 was 62.7 s (Bormann & Saul, 2008) and 70.7 s for an earthquake with a magnitude of M_w between 7 and 7.5 (Bormann & Saul, 2008). The average high frequency duration they measured for an earthquake with a magnitude of M_w between 6 and 7 was 63.3 s (Bormann & Saul, 2009) and 78.4 s for earthquake with magnitude of M_w between 7 and 7.5 (Bormann & Saul, 2009) as well. Table 1 indicates that there is a good agreement between the high frequency duration D(s) that Bormann & Saul (2008, 2009) used and the values used in this work through corresponding magnitudes.

3. Measurements

Between 1990 and 2018, the data set included 38 earthquakes with magnitudes from 6 to 7.5 (Figure 1). The vertical broad-band seismograms for the distance between 5° and 105°, were used for these earthquakes. Since the number of Iranian broad-band seismic stations was less than 5 before 2005, only international broad-band seismological networks were used for earthquakes between 1990 and 2005. After 2005, seismic networks in Iran were equipped with tens of broad-band stations, and their data are available. All international broad-band seismograms, which are available in Incorporated Research Institutions for Seismology (IRIS) Data Service for the distance between 5° and 105°, were used together with those of Iranian Seismological Center (IRSC-IGUT) and National Broad-Band Seismic Network of Iran (BIN-IIEES). After analysis of 13800 waveforms and removing the waveforms that were unusable (because of the gap, huge error in the result, high level of noise, problems in header, timing, etc.), 4768 waveforms for 38 earthquakes dataset were used.

The magnitude was estimated at different percentages (between 10% and 90%) of the maximum high-frequency envelope amplitude as the limiting threshold of high-frequency duration for amplitude selection in order to reach the best agreement with M_w^{GCMT}. Bormann & Saul (2008) used 40 percent of the maximum high-frequency envelope amplitude as the limiting threshold to select amplitude in m_B estimation. Calculations showed that some 40 percent of the maximum high-frequency envelope amplitude (Figure 3) and its corresponding calibration function (Figure 2) of m_B for the dataset gave the best agreement in the case of the present study.

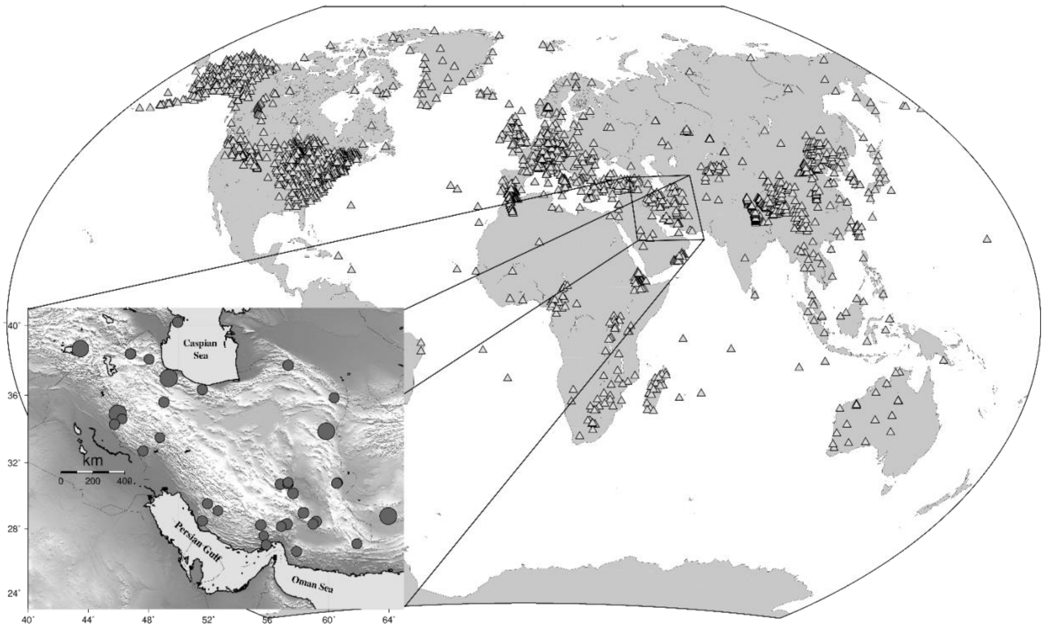

Figure 1. The distribution of earthquakes and stations used in this study. The circles and triangles show the earthquakes and stations, respectively.

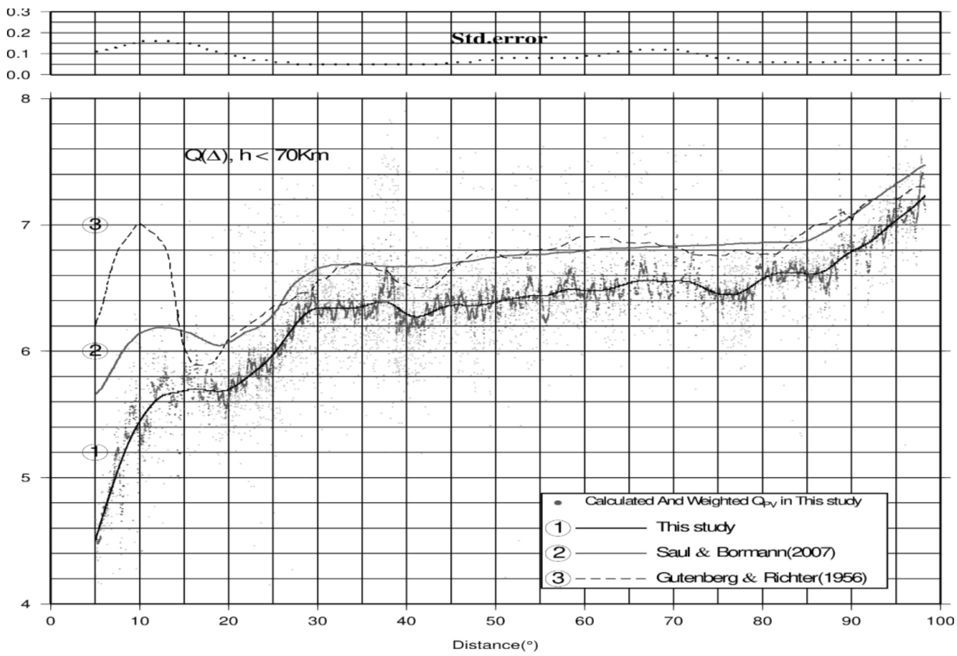

Figure 2. Calibration function of m_B (Q_{pV}) calculated in this study(b) compared to Saul & Bormann (2007), and Gutenberg & Richter (1956), with standard error for each distance(a).

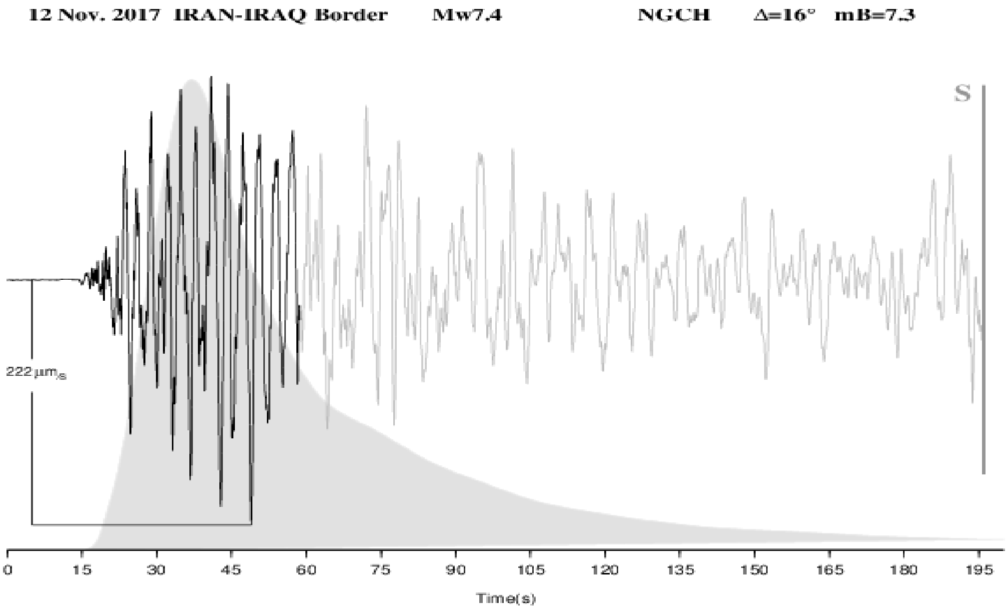

Figure 3. An example of m_B measurement for 2017 November 12 Iran-Iraq border earthquake at IR. NGCH station. High-frequency radiation, shown here as a gray-shaded curve, is used to search for maximum amplitude.

As can be seen from Figure 2, there are some deviations from the figures and calibration values (Q_{pv}) of Saul & Bormann (2007). For each distance, the calculated calibration values are smaller than those of Saul & Bormann's (2007). Therefore, global m_B calibration function was obtained (at the regional and teleseismic distance range) through the procedure of Saul & Bormann (2007) for 25 events globally distributed with magnitudes between 7 and 8.5 to ensure our procedure's accuracy. The obtained global calibration function was remarkably similar to that of Saul & Bormann (2007), which shows their procedure accuracy on a global scale. More importantly, it shows that the difference between global and regional scale (Iran plateau, in this case) is a reason for difference between m_B and M_w, were calculated for Iran's earthquake before modification.

The main purpose of this study, as mentioned above, was the rapid estimation of the magnitude that shows best agreement with M_w^{GCMT}. Therefore, as shown in Figure 4, computed magnitudes were compared with M_w^{GCMT}. As can be seen in Figure 4, m_B shows good agreement with M_w^{GCMT} for the present magnitude dataset range.

Since the m_B derived from unfiltered velocity records, it had a physical relationship to seismic energy. Moreover, a purely empirical relationship between M_w and m_B can be used as a preliminary and fast M_w estimator, M_{w*}, for better estimation of the earthquake magnitude. The relationship resulting from the use of the linear orthogonal regression of Bormann et al. (2007) method is:

$$M_w = 1.32 m_B - 2.07 \; with \; \sigma = \pm 0.18 \tag{2}$$

The good agreement between M_w and m_B for the present dataset, as well as M_{w*} and M_w can be seen in Figure 4 and Figure 5.

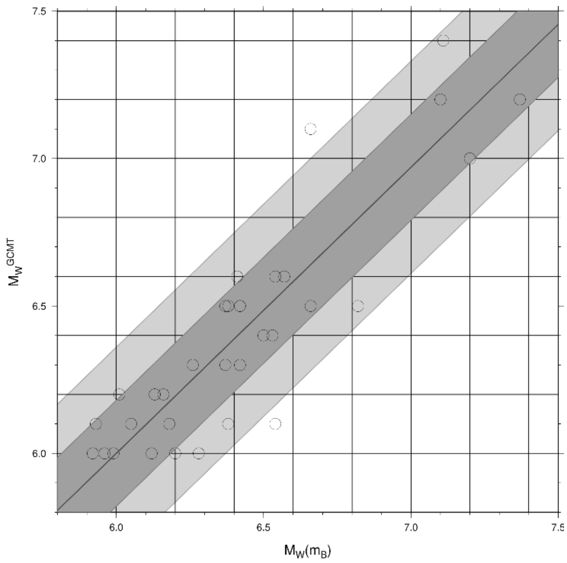

Figure 4. Comparison of estimated M_{w*}(mB), which have been computed in this study (using Equation (2)), and Mw. the 1std and 2std have been shown by gray and light gray areas, respectively.

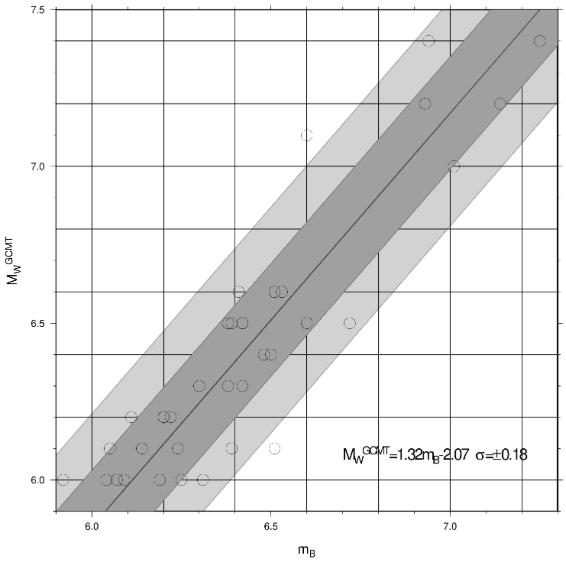

Figure 5. Comparison of estimated m_B with M_w. the 1std and 2std have been shown by gray and light gray areas, respectively.

4. Discussion

According to Bormann & Khalturin (1975) and Bormann & Wylegalla (2005), Bormann & Saul (2009) went through a procedure using peak velocity amplitudes between two adjacent zero-crossings in the P-wave train. If the peak amplitudes include more than a certain percentage of the maximum amplitude observed previously, they were summed up. The summation of selected amplitudes forms a cumulative velocity amplitude ($V_{c,n}$) by a factor of 1/2 compatible with m_B(BB) measurement, measured according to 1/2 of peak-to-trough. The $V_{c,n}$ was used as the same single amplitude in m_B(BB):

$$m_{Bc,n}(BB) = \log_{10}\left(\frac{V_{c,n}}{2\pi}\right) + Q\ (\Delta, h) \quad (3)$$

where n is the first n relevant to measured amplitudes.

They show that this magnitude is nearly equal to M_w, especially for earthquakes with a magnitude greater than 8. The present dataset consists mainly of events with magnitudes below 7 even though m_{Bc} magnitude was specifically developed for great earthquakes with $M_w \geq 7.5$. This is a magnitude range where other body-wave magnitudes like m_B (but also M_{wp}) often fail due to the saturation, especially in case of "slow" earthquake or events with exceptionally large rupture duration. One may argue about the inclusion of earthquakes with magnitudes lower than 7 in Bormann & Saul (2009) and whether this was appropriate for establishing an empirical M_w - m_{Bc} relationship. However, their data set was dominated by mostly events above M_w 7, whereas in this dataset, only seven out of 38 earthquakes fall in this range. There are not enough data to claim that the regionalized m_{Bc} as can be achieved would perform any better in case of a future large earthquake in Iran than the original m_{Bc} by Bormann & Saul (2009). Furthermore, for the determination of m_B, only the peak P-wave amplitude is measured, which is much less sensitive to the choice of the measurement time window as determined from the high-frequency envelopes (Figure 3). Even if the reported apparent rupture duration is too high, the m_B measurement should not be negatively affected as long as there is no S-wave energy within the measurement time window. However, m_{Bc} was computed for this dataset using newly developed calibration function (Q_{pv}) and the same ratios introduced by Bormann & Saul (2009) and as can be seen from Table 1 there is good agreement between calculated m_{Bc} and M_w for earthquakes with a magnitude greater than 7. Table 1 shows m_B and m_{Bc} (calculated in this study), m_{B*} (estimated by Saul & Bormann (2007) calibration values), M_w^{GCMT} and $M_w(m_B)$.

Since more than 90% of the seismicity occurs on plate margins (Wiemer, 2004), a significant majority of Saul & Bormann (2007) dataset can be located in plate boundary earthquakes. However, the earthquakes considered in this study are located in Iranian plateau on continental plates. Interplate earthquakes have lower stress drops than intraplate earthquakes (Engelder, 2014; Stein & Wysession, 2002; Lay & Wallace, 1995). Scholz et al. (1986) concluded that the stress drop for intraplate earthquakes are systematically about five times greater than that of interplate earthquakes. The most striking feature of the global stress drop variation map obtained by Allmann & Shearer (2009) was the region of extremely low stress drops along the subduction zone and plate boundaries. Besides, Iran's earthquakes show a high level of stress drop compared to subduction zones and plate boundaries earthquakes. Therefore, the stress drop of our events was more than that of Saul & Bormann (2007) events.

The stress drop is proportional to the radiated energy (Stein, 2002), so it has an effect on m_B calculation. Also, the stress drop is proportional to the moment and inversely proportional to the fault dimension cubed or the 3/2 of the fault area (Stein, 2002):

$$\Delta\sigma = c\frac{M_0}{L^3} = c\frac{M_0}{S^{3/2}} \quad (4)$$

where c is a factor depending on fault's shape. For a given magnitude, the higher the stress drop, the shorter the rupture length (Oliveira et al., 2006), and the rupture length is also proportional to the duration of pulse. As a result, high level of the stress drop leads to an increase in P-wave amplitude. Since the stress drop is high in Iran, the lower calibration function for Iran earthquakes is expected compared to the global calibration function calculated by Saul & Bormann (2007). Thus, as expected, for each distance, the calculated calibration function is lower than Saul & Bormann's (2007) calibration function.

Table 1. Network average computation for 38 Earthquakes.

Date	**D (s)**	**M_w^{GCMT}**	**m_B**	**m_{Bc}**	**M_w(mB)**	**m_{B*}**
20-Jun-90	49	7.4	6.94	7.50	7.11	6.56
6-Nov-90	52	6.5	6.60	6.70	6.66	6.69
23-Feb-94	50	6.1	6.51	6.55	6.54	6.74
24-Feb-94	70	6.3	6.38	6.45	6.37	6.68
1-Mar-94	54	6.0	5.92	6.53	5.76	6.61
4-Feb-97	74	6.5	6.39	6.70	6.38	6.68
28-Feb-97	52	6.1	6.14	6.46	6.05	6.48
10-May-97	70	7.2	6.93	7.24	7.10	6.78
14-Mar-98	70	6.6	6.53	6.64	6.57	6.76
4-Mar-99	56	6.6	6.41	6.75	6.41	6.70
6-May-99	56	6.2	6.20	6.50	6.13	6.69
25-Nov-00	51	6.5	6.42	6.77	6.42	6.79
6-Dec-00	56	7.0	7.01	7.31	7.20	6.90
22-Jun-02	72	6.5	6.72	6.74	6.82	6.75
26-Dec-03	71	6.6	6.51	6.89	6.54	6.63
28-May-04	74	6.3	6.42	6.60	6.42	6.83
22-Feb-05	64	6.4	6.50	6.78	6.53	6.51
13-Mar-05	42	6.0	6.19	6.43	6.12	6.43
28-Feb-06	59	6.0	6.09	6.36	5.99	6.56
25-Mar-06	62	5.9	5.88	6.26	5.71	6.61
31-Mar-06	56	6.1	6.05	6.52	5.93	6.51
10-Sep-08	63	6.1	6.24	6.53	6.18	6.66
20-Dec-10	67	6.5	6.42	6.70	6.42	6.69
18-Jan-11	69	7.2	7.14	7.49	7.37	6.69
27-Jan-11	76	6.2	6.11	6.55	6.01	6.42
23-Oct-11	64	7.1	6.60	6.61	6.66	6.64
11-Aug-2012 (12:23)	63	6.4	6.48	6.61	6.50	6.74
11-Aug-2012 (12:34)	70	6.5	6.38	6.60	6.37	6.93
9-Apr-13	69	6.3	6.30	6.51	6.26	6.71
11-May-13	60	6.2	6.22	6.63	6.16	6.49
18-Aug-14	70	6.2	6.20	6.41	6.13	6.95
5-Apr-17	66	6.0	6.07	6.30	5.96	6.83
12-Nov-17	43	7.4	7.25	7.50	7.52	6.77
1-Dec-17	76	6.1	6.39	6.40	6.38	6.75
12-Dec-2017 (08:42)	90	6.0	6.25	6.34	6.20	6.74
12-Dec-2017 (21:43)	71	6.0	6.04	6.25	5.92	6.73
25-Aug-18	46	6.0	6.31	6.40	6.28	6.65
25-Nov-18	70	6.3	6.25	6.56	6.20	6.72
D: Time window Duration(second) for Magnitude Computation estimated by High-frequency duration.						
M_w(m_B), m_B, m_{Bc}: Measurement based on This Study						
m_{B*}: Measurement using Bormann and Saul (2007) calibration values						

5. Conclusion

Clearly, there is a need for fast estimation of great earthquakes' magnitude using an accurate method, especially for countries such as Iran where the seismic risk is significantly high. A useful procedure to reduce the estimation time is the use of P-wave train. It leads to focusing on the methods that P-wave train is used to estimate the magnitude. Therefore, the magnitude m_B was chosen as fast and accurate estimation of great earthquakes. In addition to less complexity, the computation, which is derived from unfiltered velocity traces, associates these magnitudes with seismic energy and increases accuracy.

There was a noticeable difference between estimated m_B for 38 earthquakes in Iran and adjacent areas using Saul & Bormann's (2007) calibration function and reported magnitudes, M_w^{GCMT}. Consequently, the calibration function was modified to achieve better results.

Modification of m_B calibration function plays a vital role in the estimation of the magnitude for interplate earthquakes, such as Iran plateau earthquakes that have high stress drop compared with global scale average. However, there was a good agreement between the results of this study and those of M_w^{GCMT}. A least-square orthogonal fit between M_w and m_B allows a preliminary estimate of M_w, M_{w*}. The final purpose of this study was to modify m_B and $M_w(m_B)$ for Iranian plateau. This modification led to a high degree of accuracy for the events that occurred and can be proposed for earthquake monitoring agencies in Iran.

6. Data and Resources

Local seismograms used in this study were collected using national seismological networks IRSC-IGUT and BIN-IIEES at www.irsc.ut.ac.ir (last accessed April 2017) and www.iiees.ac.ir (last accessed April 2018), respectively. Global seismograms were obtained from the IRIS Data Management Center at www.iris.edu (last accessed April 2018). All plots were made using the Generic Mapping Tools Version 4.5.6 (www.soest.hawaii.edu/gmt; Paul Wessel and Walter H. F. Smith (1999)).

Acknowledgements

The authors cherish the memory of Peter Bormann (1939-2015) who provided this study with his innumerable comments. The authors wish to acknowledge the valuable comments of Joachim Saul that improved the manuscript. IRSC-IGUT, BIN-IIEES and IRIS should also be thanked for providing the data and waveforms used in this study. The maps and graphs were drawn with the Generic Mapping Tools (Wessel & Smith, (1991).

References

Allmann, B.P., & Shearer, P.M. (2009). Global variations of stress drop for moderate to large earthquakes. *Journal of Geophysical Research*, 114(B01), 310.

Astiz, L., Earle, P., & Shearer, P. (1996). Global stacking of broadband seismograms. *Seismological Research Letters*, 67 (4), 8–18. doi: https://doi.org/10.1785/gssrl.67.4.8

Berberian, M., & Walker, R. (2010). The Rüdbar M_w 7.3 earthquake of 1990 June 20; seismotectonic, coseismic and geomorphic displacements, and historic earthquakes of the western high-Alborz, Iran. *Geophysical Journal International*, 182(3), 1577–1602, DOI:10.1111/j.1365-246X.2010.04705.x, URL:http://dx.doi.org/10.1111/j.1365-246X.2010.04705.x.

Boatwright, J., & Choy, G.L. (1986). Teleseismic estimates of the energy radiated by shallow earthquakes. *Journal of Geophysical Research: Solid Earth*, 91(B2), 2095–2112, DOI 10.1029/JB091iB02p02095, URL http://dx.doi.org/10.1029/JB091iB02p02095.

Bormann, P., & Dewey, J. W. (2014). The new IASPEI standards for determining magnitudes from digital data and their relation to classical magnitudes. In: Bormann, P. (Ed.), New Manual of Seismological Observatory Practice 2 (NMSOP-2), Potsdam: Deutsches GeoForschungsZentrum GFZ, 1-44. https://doi.org/10.2312/GFZ.NMSOP-2_IS_3.3

Bormann, P., & Khalturin, VI. (1975). Relations between different kinds of magnitude determinations and their regional variations.in *proceedings of the xivth general assembly of the European seismological commission, trieste, sept*. 16-22, 1974, ed. H. Stiller, 27-39, Berlin. National komitee for Geodesie und Geophysik bei der Akademie der Wissenschaften der DDR.

Bormann, P., & Saul, J. (2008). The new IASPEI standard broadband magnitude mB. *Seismological Research Letters*, 79(5), 698–705.

Bormann, P., & Saul, J. (2009). A fast, non-saturating magnitude estimator for great earthquakes. *Seismological Research Letters*, 80(5), 808–816.

Bormann P., & Wylegalla, K. (2005). Quick estimator of the size of great earthquakes. *Eos, Transactions, American Geophysical Union*, 86(46), 464.

Bormann, P., Wylegalla, K., & Saul, J. (2006). Near real-time broadband body-wave magnitudes m_B and m_{Bc}: Automatic procedure for reliable magnitude estimates of strong earthquakes. In: USGS Tsunami Sources Workshop at, Menlo Park, http://walrus.wr.usgs.gov/tsunami/workshop.

Bormann, P., Liu, R., Ren, X., Gutdeutsch, R., Kaiser, D., & Castellaro, S. (2007). Chinese national network magnitudes, their relation to NEIC magnitudes, and recommendations for new IASPEI magnitude standards. *Bulletin of the Seismological Society of America*, 97(1), 114-127. doi.org/10.1785/0120060078

Chung, D.H., & Bernreuter, D.L. (1980). Regional relationships among earthquake magnitude scales. US Nuclear Regulatory Commission Lawrence Livermore Laboratory: Washington, D. C. 20, 555.

Duputel, Z., Kanamori, H., Tsai, C., Rivera, L., Meng, L., Ampuero, J., & Stock, J., (2012). The 2012 Sumatra great earthquake sequence. *Earth and Planetary Science Letters*, (351–352), 247-257. https://doi.org/10.1016/j.epsl.2012.07.017

Duputel, Z., & Hayes, G. (2012). W-phase fast source inversion for moderate to large earthquakes (1990 - 2010). *Geophysical Journal International*, 189(2), 1125–1147.

Dziewonski, A.M., Chou, T.A., & Woodhouse, J.H. (1981). Determination of earthquake source parameters from waveform data for studies of global and regional seismicity. *J. Geophysics Res.*, 86, 2825–2852, DOI 10.1029/JB086iB04p02825.

Ekström, G., Nettles, M., & Dziewonski, A.M. (2012). The global CMT project 2004-2010: Centroid-moment tensors for 13,017 earthquakes. *Phys. Earth Planet Inter.*, 200-201, 1–9, DOI 10.1016/j.pepi.2012.04.002.

Engelder, T. (2014). *Stress Regimes in the Lithosphere*. Princeton University Press, URL http://www.jstor.org/stable/j.ctt7zv82v.

Evernden, J.F. (1967). Magnitude determination at regional and near regional distances in the United States. *Bull. Seism. Soc. Am.*, 57(4):591-639.

Gutenberg, B., & Richter, C. F. (1956). Magnitude and Energy of Earthquakes. *Annals of Geophysics*, 9(1), 1-15. doi:10.4401/ag-5590.

Gutenberg, B. (1945). Magnitude determination for deep-focus earthquakes. *Bulletin of the Seismological Society of America*, 35(3), 117–130. doi:https://doi.org/10.1785/BSSA0350030117.

Hanks, T.C., & Kanamori, H. (1979). A moment magnitude scale. *J. Geophysics Res.*, 84(B5), 2348–2350.

Hayes, G., Rivera, L., & Kanamori, H. (2009). Source Inversion of the W-Phase: Real-time Implementation and Extension to Low Magnitudes. *Seismological Research Letters*, 80 (5), 817- 822. doi: https://doi.org/10.1785/gssrl.80.5.817.

IASPEI (2013). Summary of magnitude working group recommendations on standard procedures for determining earthquake magnitudes from digital data P, http://www.iaspei.org/commissions/CSOI.

Kanamori, H. (1993). W-phase. *Geophysical Research Letter*, 20 (16), SN 0094-8276, 1691-1694, URL: https://doi.org/10.1029/93GL01883

Kanamori, H., & Rivera, L. (2008). W-phase. Source inversion of w phase: speeding tsunami warning. *Geophysical Journal International*, 175(1), 222–238.

Lay, T., & Wallace, C. (1995). Modern global seismology. Academic press, ISBN: 9780127328706.

Lomax, A., & Michelini, A. (2005). Rapid determination of earthquake size for hazard warning. EOS Trans., AGU, 86(19), 185–189.

Lomax, A., & Michelini, A. (2009). M_{wpd}: A duration amplitude procedure for rapid determination of earthquake magnitude and tsunamigenic potential from p waveforms. *Geophysical Journal International*, 176(1), 200–214, https://doi.org/10.1111/j.1365246X. 2008.03974.x.

Lomax, A., Michelini, A., & Piatanesi, A. (2007). An energy duration procedure for rapid determination of earthquake magnitude and tsunamigenic potential. *Geophysical Journal International*, 170(3), 1195–1209, DOI 10.1111/j.1365-246X.2007.03469.x, URL: http://dx.doi.org/10.1111/j.1365-246X.2007.03469.x.

Newman, A.V., & Okal, E.A. (1998). Teleseismic estimates of radiated seismic energy: the e/m0 discriminant for tsunami earthquakes. *J. Geophys. Res.*, 103(11), 26 885–26 898.

Okal, E.A., & Talandier, J. (1989). M_m: A variable period mantle magnitude. *Journal of Geophysical Research: Solid Earth*, 94(B4), 4169–4193, DOI 10.1029/JB094iB04p04169, URL-http://dx.doi.org/10.1029/JB094iB04p04169.

Oliveira, C.S., Roca, A., & Goula, X. (2006). Assessing and Managing Earthquake Risk: *Geo-scientific and Engineering Knowledge for Earthquake Risk Mitigation: developments, tools, techniques (Geotechnical, Geological and Earthquake Engineering). Springer*, ISBN: 978-1-4020-3524-1.

Saul, J., & Bormann, P. (2007). Rapid estimation of earthquake size using the broadband P-wave magnitude mB. GeoForschungsZentrum Potsdam, Germany.

Scholz, C.H., Aviles, C.A., & Wesnousky, S.G. (1986). Scaling differences between large interplate and intraplate earthquakes. *Bull. Seism. Soc. Am.*, 76(1), 65–70.

Sipkin, S.A. *(1994). Rapid determination of global moment-tensor solutions. Geophysics Res. Lett.*, 21, 1667–1670.

Stein, S., & Wysession, M. (2002). An Introduction to Seismology, Earthquakes, and Earth Structure. *Wiley Blackwell*, ISBN: 978-0-86542-078-6.

Tsuboi, S. (2000). Application of M_{wp} to tsunami earthquake. *Geophysical Research Letters*, 27(19), 3105–3108, DOI 10.1029/2000GL011735, URL http://dx.doi.org/10.1029/2000GL011735.

Tsuboi, S., Abe, K., Takano, K., & Yamanaka, Y. (1995). Rapid determination of mw from broadband P waveforms. *Bulletin of the Seismological Society of America*, 85(2), 606–613. URL:http://www.bssaonline.org/content/85/2/606.abstract.

Tsuboi, S., Whitmore, PM., & Sokolowski, T.J. (1999). Application of M_{wp} to deep and teleseismic earthquakes. *Bulletin of the Seismological Society of America*, 89(5), 1345–1351.

Vassiliou, M.S., & Kanamori, H. (1982). The energy release in earthquakes. *Bull. Seism. Soc. Am.*, 72(2), 371–387.

Weinstein, S.A., & Okal, E.A. (2005). The mantle wave magnitude mm and the slowness parameter theta: five years of real-time use in the context of tsunami warning. *Bull. Seism. Soc. Am.*, 95(3), 779–799.

Wessel, P., & Smith, W.H.F. (1991). Free software helps map and display data. *EOS, Transactions American Geophysical Union*, 72(41), 441– 446.

Whitmore, P., Sokolowski, T., Tsuboi, S., & Hirshorn, B. (2002). Magnitude-dependent correction for M_{wp}. *Science of Tsunami Hazards*, 20(4), 187–192.

Wiemer, S. (2004). Earthquake statistics and earthquake prediction research.